TRB Annual Meeting

Ground Effect Flight Transit (GEFT) – Towards Trans-Modal Sustainability

--Manuscript Draft--

Full Title:	Ground Effect Flight Transit (GEFT) – Towards Trans-Modal Sustainability
Abstract:	Low aspect ratio design in ground-effect flight is the critical feature to enable the combination of ground effect flight and free flight for the non-stop transition from flight engaging railway, subway, highway, and waterway corridors. Efficient ground effect flight allows for novel applications of existing railway infrastructure for improved transportation. The non-stop transition from these corridors enables new approaches to reduce the costs of transit congestion and infrastructure. A new ground effect flight transit platform (GEFT) uses a hovercraft-type cavity having aspect ratios less than 1.0 to achieve energy efficiencies more than 200% the efficiencies of contemporary automobiles and aircraft. Computational fluid dynamics (CFD) provides insight and performance trends to match vehicle specifications with corridors and applications. Applications range from commuter to trans-continental transit.
Additional Information:	
Question	**Response**
The total word count limit is 7500 words including tables. Each table equals 250 words and must be included in your count. Papers exceeding the word limit may be rejected. My word count is:	7178
Manuscript Classifications:	Aviation; Aviation System Planning AV020; Environmental Issues of Aviation AV030; Sustainability/Adaptation/Resilience; New Users of Shared Airspace AV095; Public Transportation; Planning and Development AP025; Land Use and Development; Rail; Passenger Rail Transportation AR010; Rail; Rail Transit Infrastructure Design and Maintenance AR060; Transit; Sustainability and Resilience; Transportation and Sustainability; Alternative Transportation Fuels and Technologies AMS40; Electric and Hybrid-Electric Vehicles; Advanced/Urban Air Mobility; Multi-Modal Transportation Systems; New/Alternative Energy-Powered Aircraft
Manuscript Number:	
Article Type:	Presentation and Publication
Order of Authors:	Adam B. Suppes, PhD
	Galen Suppes, Ph.D.

Ground Effect Flight Transit (GEFT) – Towards Trans-Modal Sustainability

Adam B. Suppes, PhD
Senior Research Engineer
HS-Drone, LLC
Charlottesville, VA, 22911
Email: asuppes@seas.upenn.edu
ORCiD: 0009-0007-5719-7907

Galen J. Suppes, PhD, P.E.
Chief Engineer
HS-Drone, LLC
Charlottesville, VA 22911
Email: suppesg@hs-drone.com
ORCiD: 0000-0002-3076-4955

Word count: 5428 + 7 tables

Submitted July 31, 2024

Abstract

Low aspect ratio design in ground-effect flight is the critical feature to enable the combination of ground effect flight and free flight for the non-stop transition from flight engaging railway, subway, highway, and waterway corridors. Efficient ground effect flight allows for novel applications of existing railway infrastructure for improved transportation. The non-stop transition from these corridors enables new approaches to reduce the costs of transit congestion and infrastructure. A new ground effect flight transit platform (GEFT) uses a hovercraft-type cavity having aspect ratios less than 1.0 to achieve energy efficiencies more than 200% the efficiencies of contemporary automobiles and aircraft. Computational fluid dynamics (CFD) provides insight and performance trends to match vehicle specifications with corridors and applications. Applications range from commuter to trans-continental transit.

Keywords

Efficiency, sustainability, infrastructure, time, lift, drag

Introduction

Low aspect ratio ground effect vehicles are capable of transit over existing railway, subway, highway, and waterway corridors with free flight as a transition over rough terrain. A new ground effect flight transit platform (GEFT) is able to deliver efficiency in this low aspect ratio design while using existing infrastructure to provide new paths of evolution for sustainability, as well as lower energy, time-value-of-money, and infrastructure costs. GEFT are lifting-body vehicles such as that illustrated by Figure 1.

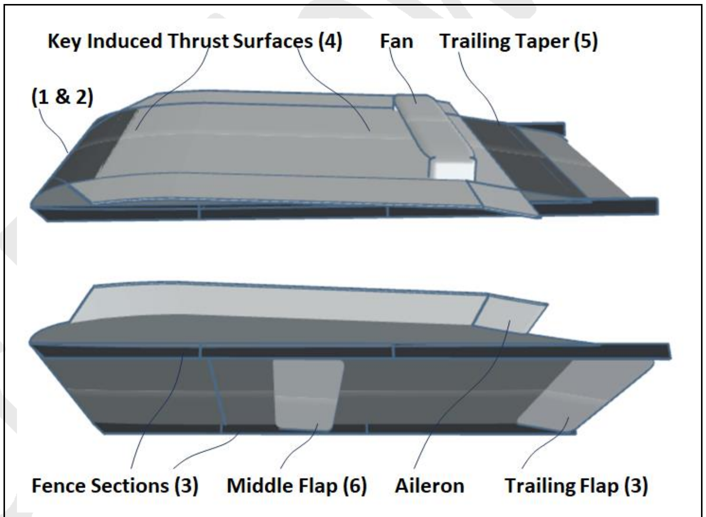

Figure 1. Digital prototype illustrating innovations.

A goal of the research reported in this paper is to demonstrate increases in energy efficiency over concurrent aircraft and railcar technologies for passengers and light cargo; and in attaining that goal, to decisively reduce energy costs to being less than transit money-value-of-time and infrastructure costs. A further goal is to identify a path forward to substantially reduce time and infrastructure costs.

The clearance ratio (i.e., ratio of vehicle clearance to lifting body thickness) is a key operating parameter that impacts efficiency for ground-effect flight, with lower clearance ratios providing higher energy efficiencies. The smooth level surface of railway tracks enables lower clearance ratios while choppy water would demand higher clearance ratios. Toward the goal of trans-modal operation an understanding of matching the vehicle design with transit corridor is a critical step in research and development. The initial focus is on railway travel.

This paper prioritizes matching vehicle design with application, building on previously established benchmarks [1]. Table 1 includes GEFT vehicles, prior to June of 2024, in a comparison of energy efficiency benchmarks; it does not match vehicle design with corridors or payloads.

Table 1. Comparison of GEFT energy efficiencies with contemporary benchmarks [1-5].

Contemporary Vehicles	**Statistical (Btu/passenger-mile)**	**L/D**	**Estimated (Btu/passenger-mile)**
Multicopters		5	6459
Helicopter		6	5383
Cessna 172		11	2936
Short-Haul Flight	3472		
Car	2569		
Airliner	2153	15	
U.S. Commuter Rail	1583		
Bus	1389		
Ferry	264		
GEFT Vehicles	**Aspect Ratio (camber)**	**L/D**	
- flap only	0.75 (FS)	5.2	6211
- aft source	0.75 (FS)	20	1615
- pair of fences	0.78 (0.02)	42	769
- two fence pairs, Source	0.78 (0.02)	62	521
- pair of fences, no wing	0.5 (0.02)	53	609

Background

To meet clean energy goals within the United States and other markets, public transit is a critical infrastructure for development. Improvements in electric vehicles for single transport efficiency will only improve emissions by a small margin and will continue to require extensive expenses in infrastructure costs. Compared to electric vehicles, ferries and national rail are already more energy efficient methods of transportation, with airliners not far behind [3]. Developments in electric aircraft pose increased energy efficiency greater than electric vehicles. To obtain the greatest impact on energy efficiency, it is necessary to target improvements to public transportation. This paper outlines the advancement of rail infrastructure to provide more efficient transportation utilizing existing infrastructure to improve the sustainability and resilience of public transportation in society.

An active area of research for sustainable, clean transportation is into the development of air taxis. A variety of air taxi designs are in development, including designs based on helicopter archetypes and small airplane archetypes [6]. However, a number of factors impact the development of a sustainable system. Helicopters, and air taxis based on rotary blade concepts, have approximately one third of the L/D, lift-to-drag, efficiency or airliner planes, which severely limits the potential energy efficiency of their designs and incorporation of clean energy sources [2]. Similarly, from a design standpoint, air taxis based on traditional airplane structures require low aspect ratios, AR, for operation within cities and crowded locations [7]. The impact of low aspect ratios compatible with use on highways also has a detrimental impact on contemporary airframe LD efficiency, also resulting in approximately one third the efficiency of commercial airliners.

Additional infrastructure requirements limit the potential impact and development of sustainable and reliable air taxis:

- Addition of new infrastructure is a problem due to lack of space and already mounting burdens to maintain existing infrastructure.

- Meeting capacity needs/wants with flight of large numbers of air taxis over cities is problematic in many ways.
    - Regulations are required for direction of transit.
    - Air downflow is problematic for vehicles and pedestrians.
    - Landing locations and sites have limited surface area.
- Traffic congestion, first/last mile costs, time/cost of transfer between modes, and security needs for larger passenger vehicles are **all** in need of resolution.

Intermodal ground-effect flight vehicles provide a solution to all these.

Intermodal ground-effect flight vehicles travel at exceptionally high efficiency on railway, highways, greenways, and waterways (cumulatively, “corridors”) while having the ability of free flight connectivity between corridors.

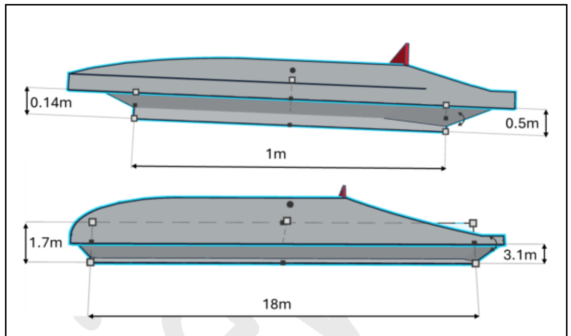

Figure 2. Key dimensions of 3D digital prototypes.

Accessibility to society - Railroad tracks, both in use and abandoned, have pre-existing access to major cities and points of interest without the requiring construction of new infrastructure. Passenger rail needs greater efficiency, with the majority of use in the northeast corridor.

Within the last 30 years, 30% of the US railroads have been abandoned or sold to short service rail services [8].

Only 1/7th of all railroads in use operates with passenger rail [8, 9]. Passenger rail operates with government subsidies and often rings railroads from freight outside of the northeast corridor. Freight is dominant. These are maintained to lower standards than passenger rails - safety and quality. Multiple attempts to fund high rail have failed in the United States - primary reasons for failure included significant cost compared to other countries due to greater distances between cities and lack of support for the general populace which prefers air and car travel for infrastructure investments. Improvements in efficiency, speed, and cost is critical to reinvigorating railway usage for passengers.

Most recent attempts at developing high speed rail options include hyperloop and maglev technologies. A major hurdle in the development of these technologies includes railroad tolerances. The tracks for hyperloop and maglev technologies for high speeds often require deviations in millimeter heights or less [10-12]. To accommodate this, independent tracks are generally constructed at high cost with high upkeep; these technologies are unable to use existing railway infrastructure with minimal changes to maintenance. The development of efficient ground effect transport options would allow for flight guided by railways, but not in contact. Therefore, they do not require high tolerances.

Base Case Fuselage – The Figure 1 prototype meets the criterion of having an aspect ratio less than 1.0. However, the thickness ratio is too low for a railcar at the width of a standard railway corridor. The height is suitable for parcels and some freight transit.

Simply increasing the thickness of the design results in an increased pitch of the lift span, and a pitch greater than 1° results in incremental L/D less than 60. To simplify scaleup, a horizontal Lift Span allows for a focus on the taper behind the Source as the emphasis for adjusting the design. Ultimately, each fuselage thickness design and length should be independently optimized.

Figure 3 summarizes the airfoils and dimension terminology used in this study. The Airfoil A design achieved the highest efficiency in Table 1 benchmark studies. The Airfoil B design is a simple camber filled to achieve a horizontal lower surface at the cruising condition as well as a horizontal Lift Span as part of distributed propulsion. Airfoils B-E include the base case designs that are scaled by increasing the thickness which increases the thickness ratio (i.e., ratio of thickness to chord) with minimal if any pitch on lower and upper surfaces. In three dimensional studies, airfoils B-E include side fences at the same depth, or lower, than the trailing flap, as seen in figure 2.

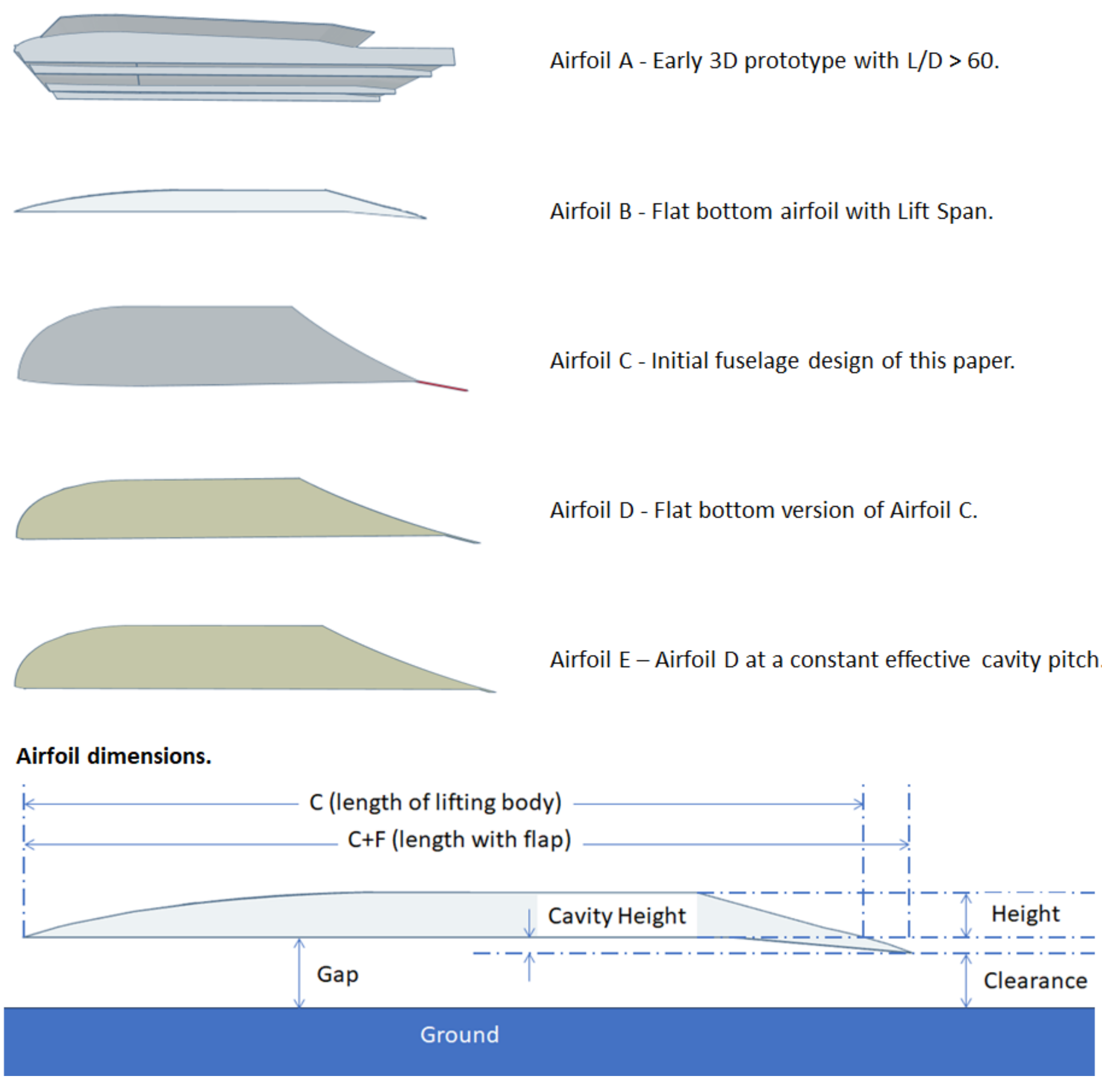

Figure 3. Cross-sections Airfoils studied in this paper [13].

Methods

Digital Experiments - OpenFoam and Simflow CFD software were used to simulate digital prototypes prepared as STL files. CFD has been shown to reliably simulate aerodynamic flight [14-16]. Two-dimensional (2D) simulations were used to identify trends in performance while 3D simulations were performed on the final prototypes and for trends which require aspect ratio parameters. Unless otherwise reported, the scale chord of the STLs were 1 m, the fluid was air at 1 atm pressure, and the free stream velocity was 40 m/s.

The ground was simulated as a lower boundary condition having a velocity equal to the free stream air. Propulsion sources were simulated as cubical geometries that generated horizontal velocities based on the power setting. Source settings are not directly related to energy requirements or efficiencies in this paper. Source input has units of m^4/s^2.

Results from CFD simulations (i.e., experiments) include: lift coefficients (C_l), drag coefficients (C_d), L/D (equal to C_l/C_d), pressure profile images, and velocity profile images. Pres:Visc drag ratio is calculated from dividing the pressure drag component by the viscous drag component. Flow around wheels on the vehicle is not considered under the assumption that air flow can be streamlined between fences and wheels.

All pressure profiles of this paper use a pressure color plot with equal positive and negative magnitudes. Vivid red is always higher pressure (relative to free stream pressure), vivid blue is lower pressure, and lime green is free stream pressure. The pressure is reported as P/ρ in units of m^2/s^2.

2D CFD studies are referred to as “airfoil studies”. In 3D studies, the use of fences allows the performance of lower surface pressures of 3D prototypes to approach the pressures and performance of the 2D airfoils. The 2D airfoils were used to refine designs with subsequent verification with 3D prototypes.

The Results section follows the sequence of studies in this research; wherein, both that sequence conveys the basis on which design choices were made. The goal is both an understanding and a development towards conclusions.

Results

Preliminary 2D Simulations – Performances of preliminary airfoil studies are summarized in Table 2. The L/D efficiency of the 0.20 t/c airfoil C ranged from 14.7 to 15.2 without a source, which is considerably less than lower t/c airfoils. Figure 4 provides the pressure profiles for the Airfoil C design. L/D efficiencies less than 30 are due to boundary layer separation above the trailing taper as evident by the pressure profiles of Figure 4 as low-pressure swirls behind the trailing taper.

The plot of L/D versus Source setting of Figure 5 illustrates two distinct trend lines in performance, one with boundary layer separation at lower source settings, less than $S=3m^4/s^2$, and one of higher L/D at higher source settings.

Table 2 – Preliminary simulation results based on Airfoils C.

Source	Clearance	t/c (with Flap)	L/D	cl	cd	Pres:Visc Drag Ratio
Airfoil C						
0	0.0036	0.10 (0.176)	47.1	1.32	0.028	
2.5	"	"	68.1	1.36	0.020	3.19
5	"	"	98.5	1.40	0.014	1.49
	0.0054	0.10 (0.176)	45.7	1.28	0.028	
	"	"	66.9	1.33	0.020	3.08
	"	"	96.8	1.37	0.014	
0	0.0036	0.20 (0.06)	15.2	1.45	0.095	
2.5	"	"	16.3	1.55	0.095	35.02
5	"	"	32.5	1.63	0.050	
10	"	"	49.4	1.72	0.035	
1	"	"	15.8	1.49	0.094	
Airfoil C with Smoothed Upper Surface Taper						
0	0.0036	0.20 (0.027)	16.5	1.45	0.088	
2.5	"	"	33.5	1.60	0.048	
5	"	"	41.9	1.65	0.039	
10	"	"	64.7	1.73	0.027	2.62
0	0.0072	0.20 (0.027)	14.7	1.10	0.075	
2.5	"	"	33.0	1.27	0.039	
5	"	"	41.7	1.33	0.032	5.57
10	"	"	64.4	1.41	0.022	2.50

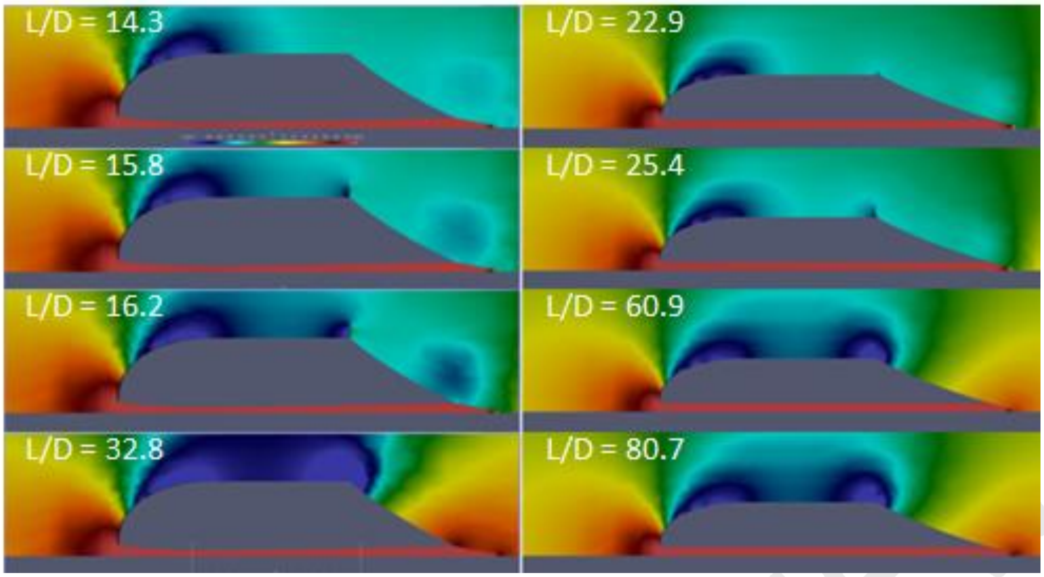

Figure 4. Pressure profiles for Airfoils C (left) and E (right) at Source settings of 0, 1, 2.5, and 5 m^4/s^2 (top to bottom).

The Source discharge is able to prevent boundary layer separation. The likely mechanism is the generation of higher discharge pressures that more-effectively fill the void of air created by the sweep of the lifting body behind the trailing taper's surface.

Figure 5 superimposes the L/D of airfoils at 0.1 and 0.2 t/c as well as a smoothed tapered airfoils on the 0.2t/c. By smoothing the taper of Airfoil C to a taper like Airfoil D, the L/D efficiency increases; the boundary layer separation is severe but alleviated at lower Source settings.

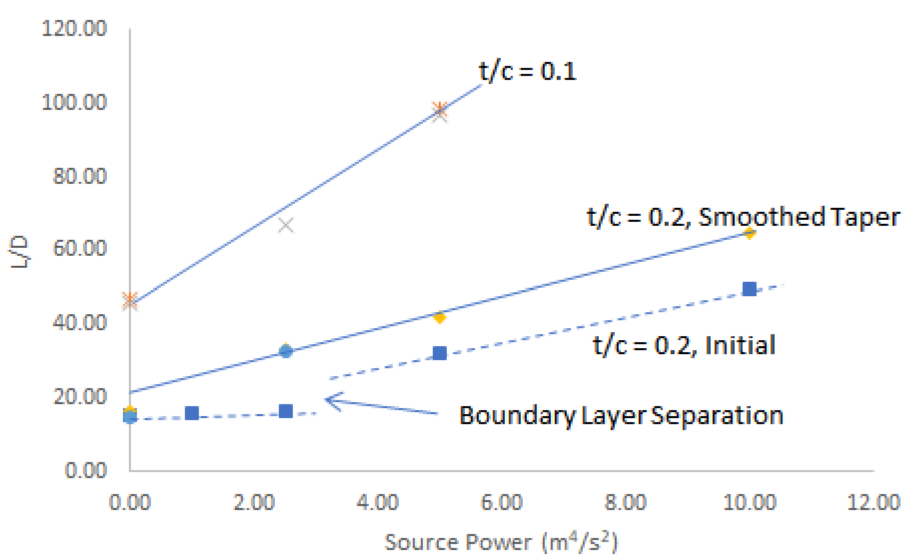

Figure 5. L/D efficiencies versus source setting for Airfoil C and Airfoil D.

Airfoil D has both a smoothed taper and a horizontal lower surface up to the trailing flap. Simulation results are summarized by Table 3 and Figures 6, 7, and 8. These data illustrate that a lower t/c of 0.14 further reduces the severity of the boundary layer separation with a Source setting of 1.0 m^4/s^2 overcoming the boundary layer separation.

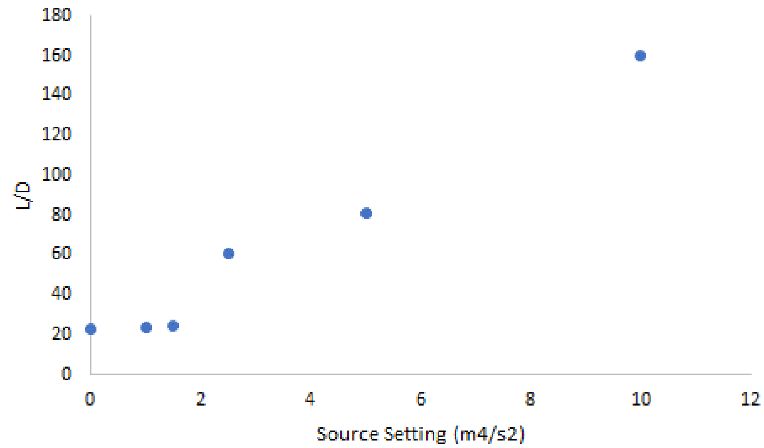

Figure 6. L/D versus source setting for Airfoil D at a 0.15 t/c.

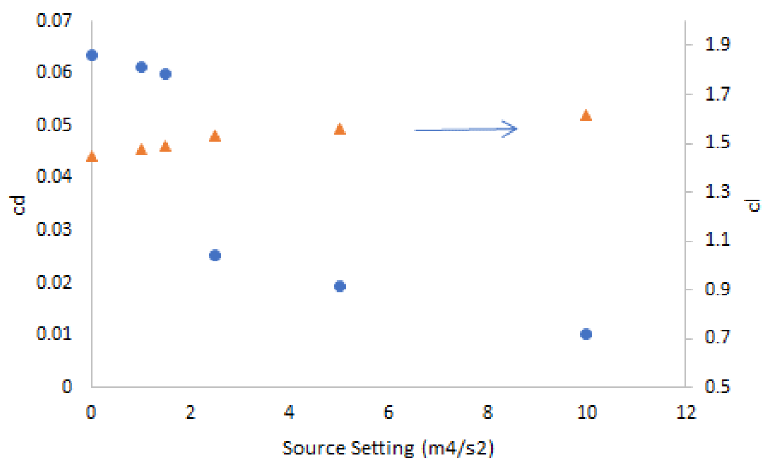

Figure 7. Lift (triangle) and drag (circle) coefficients for Airfoil D.

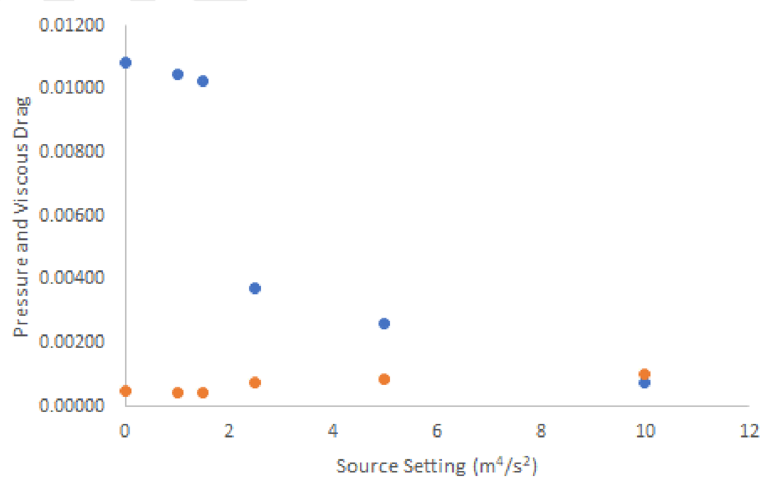

Figure 8. Pressure vs viscous drags for Airfoil D. Blue is pressure drag.

Table 3 – Summary of Airfoil D performance.

Source	Clearance (m)	t/c	L/D	cl	cd	Pres:Visc Drag Ratio
0	0.0036	0.16	19.7	1.41	0.072	
2.5			41.8	1.51	0.036	
5		**Flap**	53.1	1.55	0.029	4.71
10		0.027	86.2	1.61	0.019	1.82
0	0.01	0.15	19.9	1.28	0.064	23.53
2.5			47.0	1.40	0.030	5.66
5		**Flap**	58.5	1.45	0.025	3.73
10		0.027	89.1	1.50	0.017	1.53
1			40.6	1.37	0.034	7.57
FLAT LOWER SURFACE						
S	**Clearance**	**t/c**	**L/D**	**Cl**	**Cd**	**Pres:Visc Drag Ratio**
0	0.01	0.14	22.9	1.45	0.063	22.72
2.5			60.8	1.53	0.025	4.83
5		**Flap**	80.8	1.56	0.019	3.11
10		0.093	160.2	1.61	0.010	0.77
1			24.1	1.48	0.061	22.61
1.5			24.8	1.49	0.060	22.51

The smooth continuous curve on trailing tapers reduces the Source power needed to overcome boundary layer separation. This trend indicates the upper surface of the flap may be more important than the lower surface for airfoils to prevent boundary layer separation. Boundary layer separation is caused by the increased rate at which a void of air is created by tapers of higher pitch.

The trends of Figures 7 and 8 identify the following aspects of the boundary layer separation on Airfoil D:

- Lift coefficients through the boundary layer separation have a consistent trend. It is likely due to the predominant lift being provided by the lower surface, where the boundary layer separation has minimal impact.
- The boundary layer separation primarily lowers L/D due to the increase in form drag.
- Boundary layer separation increases form drag by reducing pressures behind the taper. Lower pressures above a surface of positive pitch create form drag.
- Boundary layer separation increases viscous drag consistent with literature values of turbulent viscosity coefficients being about 5X laminar viscosity coefficients and where the transition from laminar to turbulent viscosity is over 10% to 20% of the airfoils surface.
- After alleviating boundary layer separation, the Source continues to decrease form drag due to a continuously increasing pressure with increasing Source setting above the trailing section taper.

Understanding Impact of Clearance Ratio on L/D Efficiency – An understanding of how clearance ratio (CR) impacts L/D efficiency starts with a clear description as provided by Figure 3 and further described below:

- Clearance is the distance of closest approach of an airfoil to the ground.
- Gap is the distance of the lowest part of the lifting body, exclusive of trailing flaps and fences, from the ground.
- The Gap Ratio is the ratio of the closest approach of the lifting body to the ground divided by the lifting body thickness.
- 2D airfoils do not account for cavity fences with the clearance being set by a flap, if present. They typically exhibit the closest approach to the ground at the trailing edge of the flap.
- For 3D simulations with both a flap and fences, a flap clearance with the ground may be different than the clearance and may be specified as a % Flap, the percentage of the fenced vertical region covered by the flap, or as the flap clearance.

Also, while the t/c, flap clearance, and fence clearance impact L/D, at higher L/D the effective pitch of the cavity has the greatest impact, where:

- The effective cavity pitch is the rise (i.e., fall) over run of the lower surface decreases where higher pressures are formed and expressed on the lifting body.
- At a constant cavity pressure, the L/D contribution from the lower surface, as weighted by surface area, is equal to $57/\alpha_{eff}$ where α_{eff} is the effective pitch of the cavity in degrees and is often best estimated as the pitch of the straight line going through leading edge and trailing edge stagnation points.

Therefore, results of Figure 6 are misleading in regard to impact of t/c on L/D, since the effective pitch of the cavity changes with t/c. Airfoil E was defined under the constraint of having a distance between the lifting body’s lower surface and the flaps trailing edge; this distance was kept as a constant variable as the airfoil’s t/c was changed. The Airfoil E results with this constant variable are shown in Table 4 and a partial graphic summary of pressure profiles by Figure 9.

Table 4 Performance data of Airfoil E having a constant effective cavity pitch. Length of flat-bottom fuselage is 1.68m, flap is 0.01m lower than fuselage.

Clearance	t/c	S	L/D	Cl	Cd	Pres:Visc Drag Ratio
0.25	0.134	0	6.5	0.411	0.0590	14.56
		5	41.8	1.005	0.0179	2.91
		10	73.7	1.124	0.0081	1.12
		15	147.7	1.203	-0.0001	-0.01
0.25	0.089	0	29.1	0.589	0.0151	2.95
		5	61.9	0.734	0.0055	0.86
		10	135.4	0.803	-0.0016	-0.21
0.25	0.045	0	33.2	0.350	0.0052	0.97
		5	63.7	0.418	-0.0001	-0.01
		10	108.7	0.447	-0.0039	-0.48
0.25	0.012	0	30.6	0.201	0.0009	0.15
		5	37.6	0.246	-0.0006	-0.08
		10	37.5	0.264	-0.0016	-0.18
2.5	0.045	0	24.8	0.265	0.0055	1.05
0.01	0.045	0	89.0	0.673	0.0042	1.22
		5	197.7	0.724	-0.0010	-0.21
		10	693.4	0.740	-0.0048	-0.82

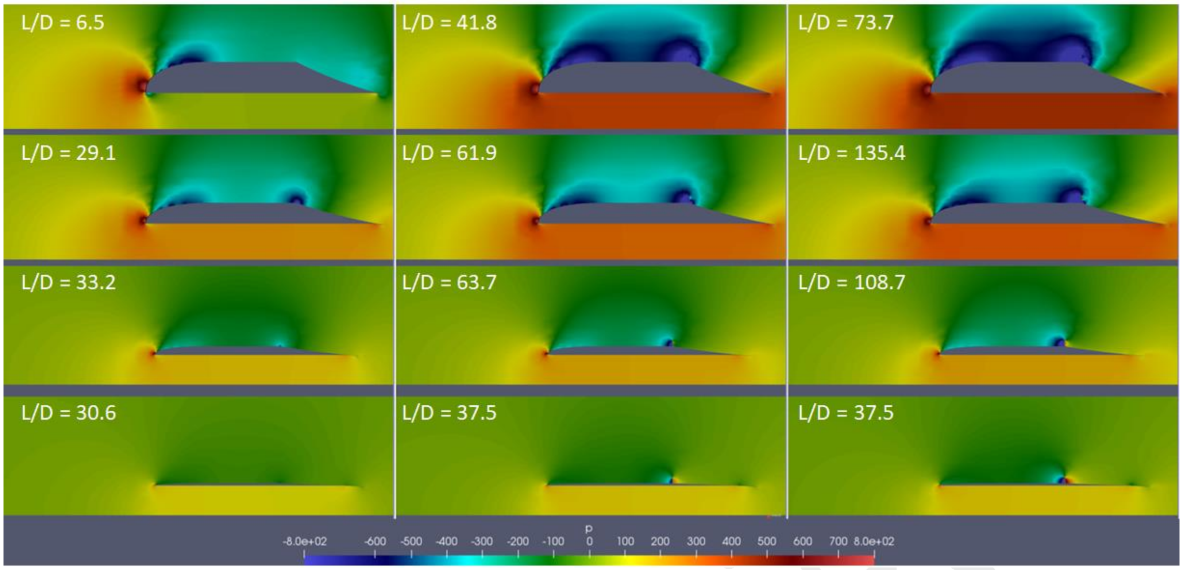

Figure 9. Pressure profiles for Airfoil E at Source settings of 0, 2.5, and 5 m^4/s^2 per the Table 4 data.

Figure 9 illustrates the following trends:

- By eliminating the cavity as a source of low L/D due to an effective pitch greater than 2°, increased L/D are realized, even at higher clearances.
- Leading edge stagnation regions increase in severity with increasing airfoil thickness, the thinner airfoils have lower cavity pressures with lower L/D due to dissipation of the forward stagnation pressures through the clearance.
- Robust trailing edge stagnation regions in combination with robust leading edge stagnation regions lead to the highest cavity pressures. The trailing stagnation region is a result of air originating from upper and lower surfaces colliding behind the trailing edge, and the higher the velocity of air along the upper surface of the trailing taper, the greater the pressures and expanse of the trailing stagnation region.

Importance of Leading-Edge Stagnation Region – Figure 9 illustrates the importance of leading-edge stagnation regions. Table 5 summarizes studies at different free stream velocities for the 0.045 t/c airfoil of Table 4. Higher velocities increase the robustness of the leading-edge stagnation region, leading to higher L/D due to the more-robust stagnation regions and respective reduced depletion of the impact on cavity pressures. Table 6 summarizes the maximum pressure realized at the different velocities with Figure 10 providing pressure profiles.

Table 5. Impact of free stream velocity on L/D for Airfoil E at t/c=0.045 and clearance ratio=0.04 for an airfoil of chord 1.68m and the flap extending 0.01m lower than the fuselage.

U (m/s)	S (m^4/s^2)	L/D	Drag Ratio (pressure:viscous)
40 m/s	0	59.4	0.98
80 m/s	0	66.0	1.21
120 m/s	0	67.6	1.27
160 m/s	0	68.8	1.31

Table 6. Maximum pressure as at the forward stagnation point for Airfoil E at t/c=0.045 and clearance ratio=0.25 for an airfoil of chord 1.68m and the flap extending 0.01m lower than the fuselage. U is free stream velocity.

t/c	U (m/s)	$P/\rho = 0.5\ U^2$	P_{max}
0.134	40	800	826
0.089	40	800	820
0.045	40	800	809
0.012	40	800	656
0.045	80	3,200	3,240
0.045	120	7,200	7,300
0.045	160	12,800	12,980

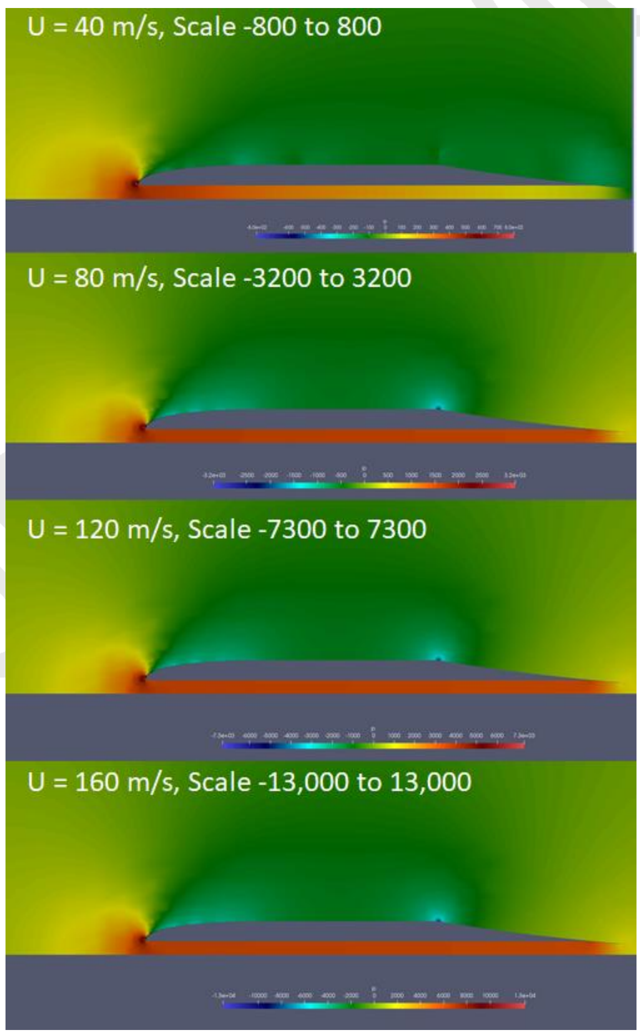

Figure 10. Pressure profiles of Airfoil E at t/c = 0.045.

Per Table 6, while in free flight the maximum pressure of the forward stagnation point readily dissipates below air's dynamic pressure, GEFT airfoils of reasonable thickness realize air's dynamic pressure at the forward stagnation region.

Figure 11 compares expanded views of the forward stagnation region of Airfoils E and B. The stagnation point, and respective highest pressure, for Airfoil B is on the lower horizontal surface where the highest pressures exhibit no form drag and have less upward dissipation. The positive pitch at the Airfoil E stagnation point leads to form drag. Under certain circumstances, the forward stagnation point of Airfoil E migrates above the leading edge with even greater form drag. Due to this, Airfoil E exhibits superior performance in ground-effect flight for GEFT.

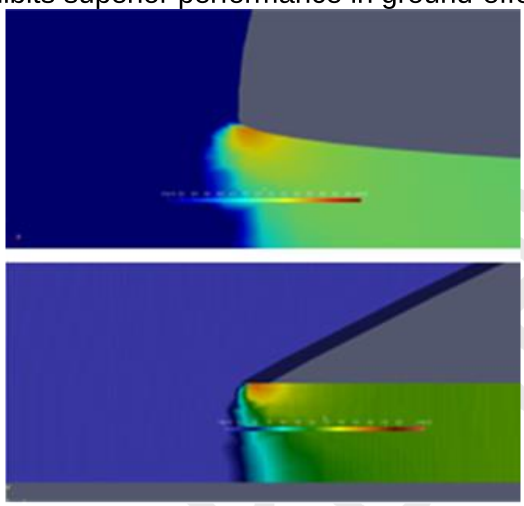

Figure 11. Expanded views and pressure profile scales of leading-edge stagnation points for Airfoils E and B.

Airfoil A was selected for initial studies due to similarity with airfoils exhibiting good performance in free flight. The optimization criteria for only ground-effect flight, only free flight, and various mixes of ground-effect and free flight are different. Studies beyond pure ground effect flight are beyond the scope of the paper except to identify that the aircraft are capable of free flight; albeit at much lower L/D efficiencies than in ground-effect flight and contemporary aircraft which use significantly wider aspect ratios.

3D Simulations – While 2D airfoil simulations do not account for lateral loss of lift pressures, 3D prototypes of GEFT use cavity fences to block losses.

Figure 12 presents the impact of fences on the L/D in a 3D model of airfoil C. An important function of the fences is to assist the propagation of high pressures from the trailing stagnation points forward through the cavity to increase lift forces. An important point of optimization: while fences may improve L/D while increasing gap ratios, after a certain height, the fences provide diminishing returns as the cavity increases in volume. In this extreme, preventing the lateral loss of pressures is not as beneficial for improving L/D efficiency but continues to have noticeable benefit over the lack of fences. Table 7 provides the data and force coefficients for Figure 12's data.

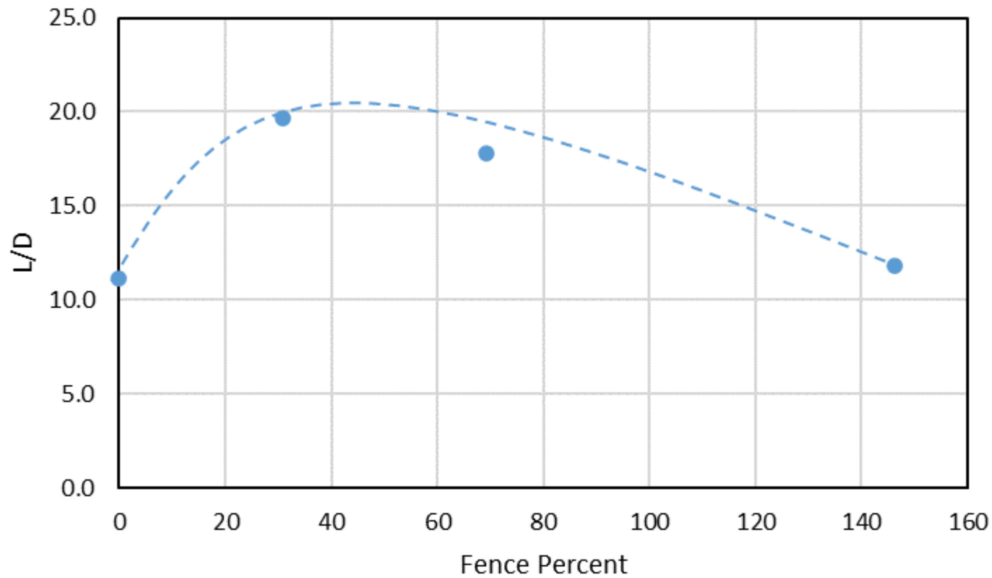

Figure 12. Impact of fence size on L/D at a clearance ratio of 0.2. Data is from a 6.4m long model of 0.62t/c airfoil C with a width of 4.8m with fence percent defined as the height of the fence normalized to the height of the airfoil.

Table 7. Impact of fence height on lift characteristics of flying railcars.

U (m/s)	Clearance Ratio	Gap Ratio	Fence Percent	C_l	C_d	L/D
40	0.2	0.2	0	1.88	0.168	11.2
40	0.2	0.51	31	6.45	0.328	19.7
40	0.2	0.90	69	9.90	0.556	17.8
40	0.2	1.67	146	12.20	1.030	11.8

Fences may be simulated with increasingly lower clearance ratios, including values such as 0.02. Wheels and skis allow reasonable application of low clearances by absorbing slight contact with the ground during flight over rails, highways, or waterways without major disturbances to flight.

Figures 13 and 14 investigate the impact of adding sources to the upper sources prior to the trailing taper on flying railcars of Airfoils B and E, each with a flap percent of 50% and 0.04 clearance ratio. Figure 13, based on Airfoil B, has a t/c of 0.7 with a length of 1m which highlights the beneficial impact of ground effect flight technologies, but lacks the conditions to be a full passenger vehicle. Figure 14 presents a flying railcar based on Airfoil E designed to operate on rail tracks with a width of 3.1m, a 0.1t/c, a length of 18m including the trailing flap, and sufficient height to manage passenger transit. Source impact is most notable in extending low pressures forward on the upper surface and modifying the trailing edge stagnation point to propagate higher pressures forward within the cavity.

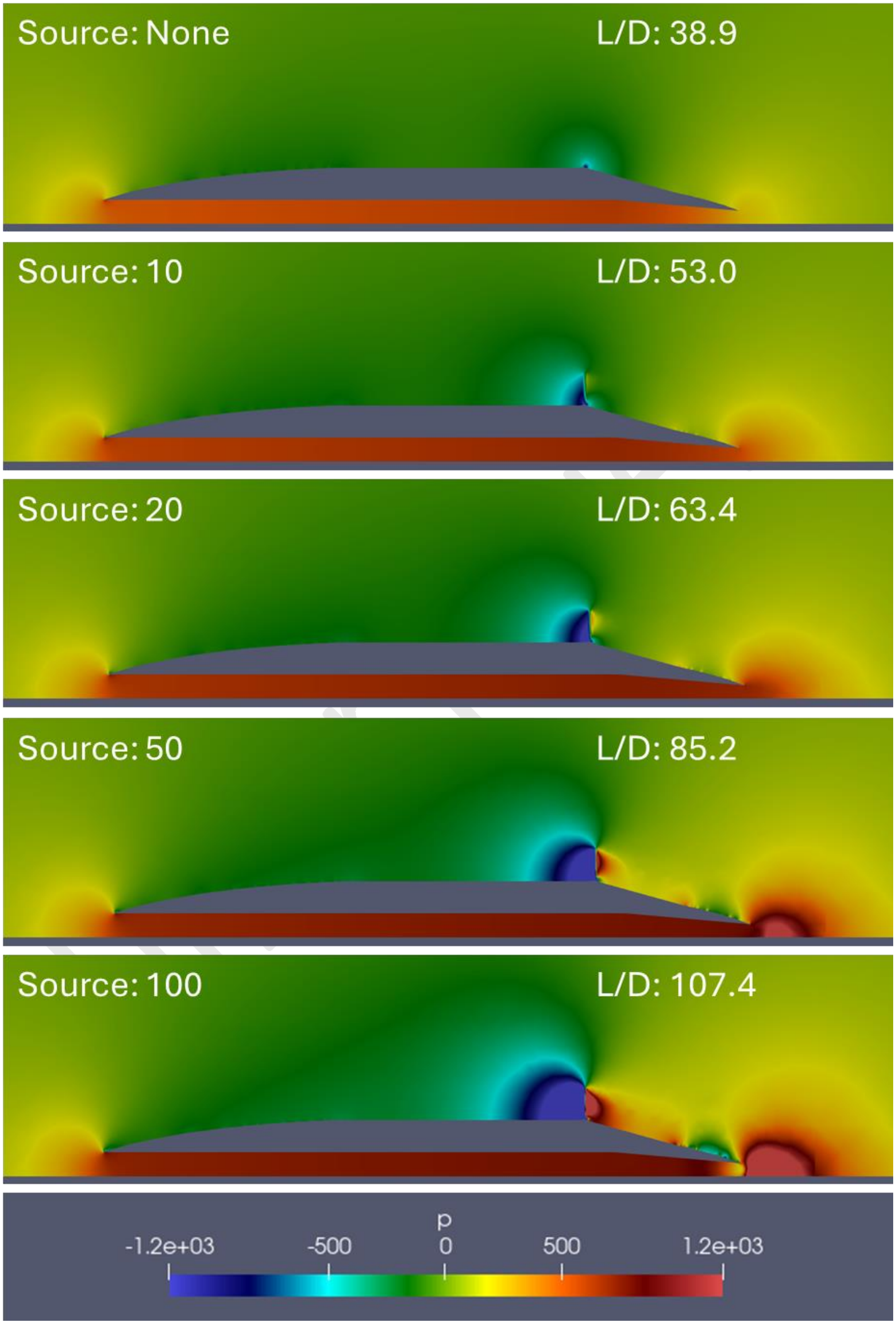

Figure 13. The impact of sources on a 3D GEFT with 1m length.

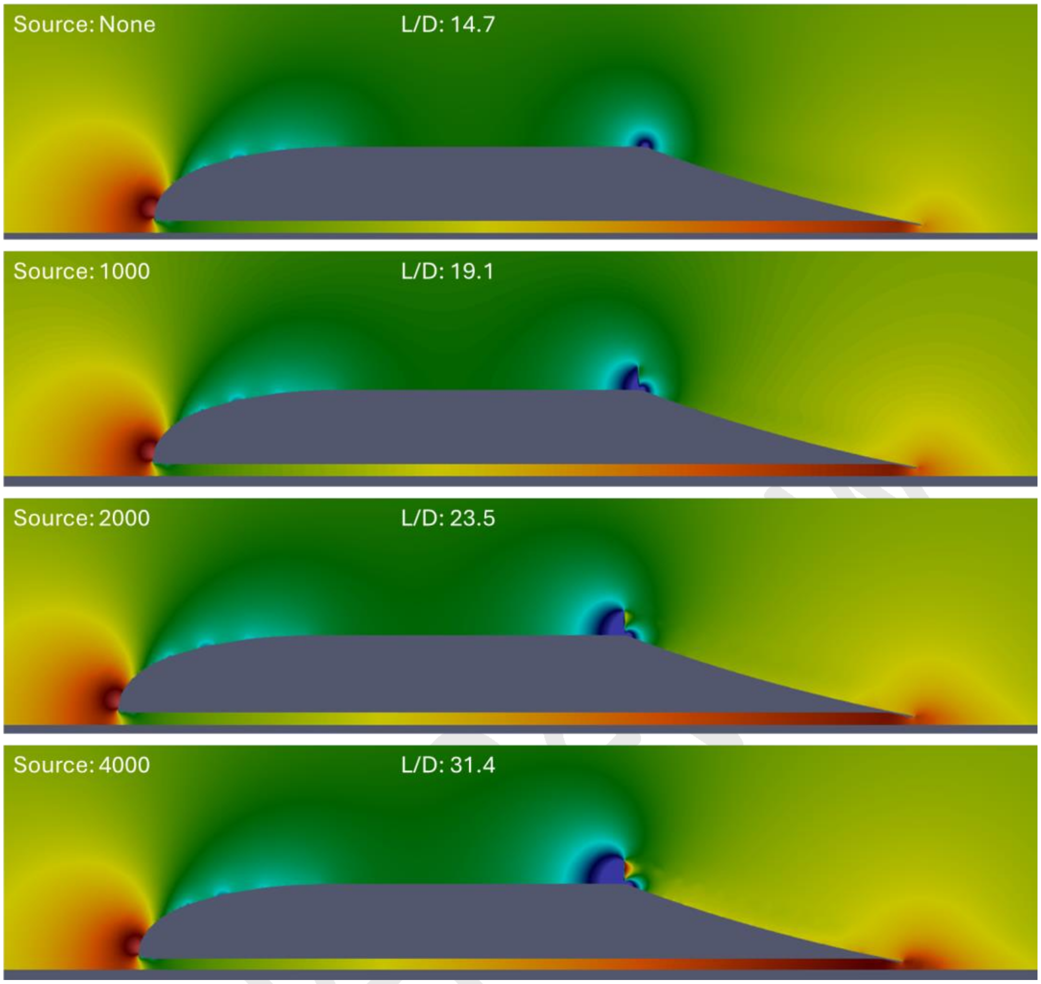

Figure 14. The impact of sources on a flying railcar designed for railway passenger transit, 18m in length.

A key point of optimization for GEFT includes design of the leading edge. An effective design transitions the leading-edge stagnation point below the leading-edge surface, as seen in Figure 13, while a non-optimized design, often with higher t/c, leaves the stagnation point in front of the airfoil, providing additional drag, as seen in Figure 14. An effective distributed propulsion source may adjust this stagnation point.

Discussion

Electric powered transportation has emerged as being favored due to the potential for low carbon footprint, diversity in source of energy, reduced noise, and zero point-source emissions. For aircraft, electric aircraft have the additional advantage of eliminating the need for aviation fuel facilities and handling. And a key enabler of electric powered aircraft is energy efficiency.

Burgeoning electric aircraft are typically of 9-passenger capacity and light weight (e.g., 10,000 lb), with L/D around 12. For instant research, ground-effect lifting bodies based on Airfoil B and Airfoil E exhibited L/D>40 in ground-effect with a narrower range of applications having L/D>50; 3.5X to 6X the efficiency of alternatives. The prototypes offer the additional advantage of operating from grid power when available from overhead lines or electrified third rails. These features substantially reduce energy costs and related environmental issues with a path for continuous improvement. Remaining transit pain points this technology may address include a) time and b) annualized infrastructure costs.

GEFT addresses annualized costs by using existing infrastructure with minimal weight nor wear and tear on that infrastructure. GEFT addresses the money value of time with high-speed non-stop transfer between corridors to avoid traffic congestion and queues at airports and railway stations.

Discussion points emerge as to which corridors are most viable with the following new benchmarks providing a starting point for that discussion:

#1. Airfoil B at: L/D=51.7, t/c=0.07, CR=0.02, GR=0.26 (GR is ratio of airfoil elevation to airfoil thickness), 50% flap, Source=0.

#2. Airfoil B at: L/D=38.9, t/c=0.07, CR=0.04, GR=0.28, 50% flap, Source=0.

#3. Airfoil B at: L/D=53, t/c=0.07, CR=0.04, GR=0.28, 50% flap, Source=10.

Corridor-specific viability considerations include:

Railways – A railcar at height of 2m operating at condition #1 with L/D of 51.7 corresponds to a length of 28m, fence-rail clearance of 4cm and car-rail clearance of 8cm. The vehicle would be able to switch between tracks for increased routing options.

Subways – A railcar could engage subway tracks at similar conditions. The restricted tunnel airflow offers additional challenges beyond this discussion.

Highways – Highways are similar to railway, except at condition #2 with fence-surface clearance of 8cm and car-surface clearance of 16cm results in an L/D=38.9. GEFT would be able to transfer between highways and railways.

Waterways – Higher clearances are needed to clear waves over water. An extrapolation to for a CR of 0.5 translates to 1m clearance with an L/D of about 15. Flight would be restricted to calm water having waves less than 2 ft in height. This option avoids the costs of bridges and enables unlimited routing options when used in combination with highways and railways.

Free Flight – Initially, free flight would be limited to a few miles at an L/D efficiency similar to a helicopter.

The above corridors represent an unprecedented capability for non-stop service from typical speeds of 90 mph (about 40 m/s) up to 360 mph. Ranges would exceed one thousand miles with the ability to use transfer hubs for longer distances. Energy costs would be 25-50% of the most-used alternative technologies with similar reductions in time and annualized infrastructure costs.

These are market-entry positions without regard to immediate improvements by:

- operating at Source settings providing the best cumulative gain in reduced drag versus loss in air-momentum thrust of the Source,
- overall optimization of vehicle sizes and design based on objectives other than maximizing energy efficiency,
- vehicle enhancement with a second pair of fences, and

- use of advanced active and passive control options to operate at lower clearances for L/D.

Applications range from commuter to intercontinental transit. Upon manufacture of vehicles, GEFT would be ready to implement with existing infrastructure without impeding current operation. GEFT can fly over obstacles to avoid them, unlike ships and trains. GEFT provide significant benefits to money value of time through avoiding congestion and reduced security times.

Conclusion

For decades, the evolution of transportation has been incremental, based on paradigms of initial technologies for business strategies (i.e., first to market) rather than breakthroughs in engineering. The consequence is a huge gap between potential versus current practices; this gap widens when considering the capabilities of technology to provide improved routing options.

The results of this paper are based on performances of digital prototypes, a research method which is both widely recognized as accurate and able to evolve much faster than physical prototypes. The advances are unique in providing major advances in the transportation pain points of: energy efficiency, environmental footprint, money value of time spent in transit congestion/queues, reduced up front infrastructure costs, and reduced annualized infrastructure costs.

Author Contributions

The authors confirm contribution to the paper as follows: study conception and design: A. Suppes and G. Suppes; data collection: A. Suppes and G. Suppes; analysis and interpretation of results: A. Suppes and G. Suppes; draft manuscript preparation: A. Suppes and G. Suppes. All authors reviewed the results and approved the final version of the manuscript.

References

[1] Suppes, A., and Suppes, G., "New Benchmarks in Ground-Effect Flight Energy Efficiency," [online database]July 10,2024https://www.researchsquare.com/article/rs-4707178/v1 [cited Jul 29, 2024].

[2] Davis, S.C., Boundy, R.G., "Transportation Energy Data Book," Oak Ridge National Laboratory, 2022.

[3] Fleck, A., "Chart: Which mode of transport is the most polluting?" *Statista,* 2024, https://www.statista.com/chart/32350/greenhouse-gas-emissions-by-mode-of-transport/

[4] McIver, J.B., "Cessna Skyhawk II / 100 Performance Assessment," 2003. http://temporal.com.au/c172.pdf

[5] Martinez-Val, R., Perez, E., and Palacin, J.F., "Historical Evolution of Air Transport Productivity and Efficiency," *Aerospace Sciences Meetings,* Vol. 43, 2005, https://doi.org/10.2514/6.2005-121

[6] Suppes, A., and Suppes, G., "Highly-Efficient Low-AR aerial vehicles in urban transit," *Proceedings of the 2014 Transportation Research Board Annual Meeting,* January, 2024,

[7] Anonymous "Lifting-line theory," 2023, https://en.wikipedia.org/w/index.php?title=Lifting-line_theory&oldid=1157579627

[8] ASCE, "2017 Infrastructure Report Card - Rail," 2017. https://www.infrastructurereportcard.org/wp-content/uploads/2017/01/Rail-Final.pdf

[9] Berman, N., "How the U.S. Rail System Works," Council on Foreign Relations, web, 2023. https://www.cfr.org/backgrounder/how-us-rail-system-works

[10] Noland, J.K., "Prospects and Challenges of the Hyperloop Transportation System: A Systematic Technology Review," *IEEE Access,* Vol. 9, No. 2021, pp. 28439-28458. 10.1109/ACCESS.2021.3057788

[11] Yaghoubi, H., Barazi, N., Kahkeshan, K., Zare, A., and Ghazanfari, H., "Technical Comparison of Maglev and Rail Rapid Transit Systems," *The 21st International Conference on Magnetically Levitated Systems and Linear Drives,* 2011, pp. 5.

[12] Deviparameswari, K., Meenakshi, S., Akshay Kumar, N., Vigneshwaran, R., Rohini Janaki, B., Vinsiya Maria, A., Keerthana, N., Surya, B., Vetrivel, M., Thianesh, U.K., Rajarajan, S., Manikandan, P., "The Effects of Ground Clearance and Boundary Layer Blockage Factor on the Aerodynamics Performance of the Hyperloop Pod and Transonic Ground-Effect Aircraft | AIAA AVIATION Forum," *AIAA Aviation Forum,* 2021, https://doi.org/10.2514/6.2021-2586

[13] Suppes, A., and Suppes, G., "Supplemental Documents in Various Stages of pre-print publication and review," 2024, https://hs-drone.com/resources

[14] Klose, B., Spedding, G., and Jacobs, G., "Direct numerical simulation of cambered airfoil aerodynamics at Re = 20,000," 2021, https://doi.org/10.48550/arXiv.2108.04910

[15] Michna, J., and Rogowski, K., "Numerical Study of the Effect of the Reynolds Number and the Turbulence Intensity on the Performance of the NACA 0018 Airfoil at the Low Reynolds Number Regime," *Processes,* Vol. 10, 2022, pp. 1004. 10.3390/pr10051004

[16] Serrano, J., Tiseira, A., García-Cuevas, L., and Varela, P., "Computational Study of the Propeller Position Effects in Wing-Mounted, Distributed Electric Propulsion with Boundary Layer

Ingestion in a 25 kg Remotely Piloted Aircraft," *Drones,* Vol. 5, 2021, pp. 56. 10.3390/drones5030056